Integral diagnosis and structural analysis of historical constructions by terrestrial laser scanning

L.J. Sánchez-Aparicio[1], S. Del Pozo[1], P. Rodríguez-Gonzálvez[1], Ángel Luis Muñoz-Nieto[1], Diego González-Aguilera[1] & Luís F. Ramos[2]

[1]*Department of Cartographic and Land Engineering. University of Salamanca, High Polytechnic School of Ávila, Hornos Caleros, 50, 05003, Ávila (Spain).*

[2]*Department of Mining Technology, Topography and Structures, Universidad de León, Avda. Astorga s/n, 24401, Ponferrada (Spain).*

[3]*ISISE, Department of Civil Engineering, University of Minho, Campus de Azurém, 4800-058 Guimarães, Portugal.*

ABSTRACT: In addition to drawing and mapping plants, cross sections and ortophotos, 3D models from terrestrial laser scanning (TLS) technology can offer relevant information for the integral diagnosis and structural analysis of buildings and constructions. Both, the metrics offered by the TLS point cloud as well as the spectral backscattered reflectance data acquired by this technology, can be used to map and evaluate structural and chemical damages of constructions in a semiautomatic and robust way. Under this basis, the present chapter attempts to offer an overview of most suitable methodologies in this regard. Specifically, a multisensory approach is proposed through which the diagnosis of the Master Gate of Saint Francisco, inside the fortress of Almeida (Portugal), has been analyzed in terms of loss of material suffered over time. The TLS point cloud was also used to extract the current resistance sections of the most damaged parts of the barrel vault, allowing the evaluation of its structural stability under different postulated casuistic: (i) in case of presenting greater material losses and; (ii) in case of a settlement of the construction.

1 INTRODUCTION

Since the appearance of the first 3D models in the beginning of this century, the use of terrestrial laser scanning (TLS) has largely spread as suitable measurement technique in the field of geomatics. TLS has become more popular due to its cheapening and its evolution in terms of its

adaptation to the demand, equipment miniaturization and greater performance of the current TLS models.

Architecture (Sánchez-Aparicio et al. 2014, Korumaz et al. 2017) and Civil Engineering (Yang, Xu, and Neumann 2018, Bautista-De Castro et al. 2018) are two of the subjects in which the application of TLS technology is most remarkable. Reverse engineering is commonly used to document historical constructions for rehabilitation and conservation works or simply to put them in value or provide support to disseminate them. The generation of orthophotos or images from uncommon points of view (Hori and Ogawa 2017) as well as their integration to virtual reality environments (Fernandez-Palacios, Morabito, and Remondino 2017) are some of the multiple applications offered by 3D point cloud models.

Thereby point clouds have become a common input in graphic engineering processes. Floor plans, cross-sections, 3D models, orthophotos, etc., derived from them bring new opportunities to Civil Engineering and Architecture, which are adapting its work procedures to improve the spatial information management.

Since the combination of the radiometric and geometric data from TLS, as well as the possibility of hybridize them other complementary thematic information provide a complete final 3D model, TLS is positioned as the first data acquisition technique for reverse engineering that offers products with which complete diagnostics of historical buildings and constructions can be performed.

On the one hand, geometrical strategies such as PCA analysis, RANSAC approach (Schnabel, Wahl, and Klein 2007) or CANUPO algorithm (Brodu and Lague 2012) are able to be applied to point clouds, allowing the extraction of planes or areas with strong material losses. In addition, a combination of those approaches offers new possibilities in the diagnosis of the conservation state of our Cultural Heritage.

On the other hand, different approaches for the spectral analysis of laser intensity data, based on the TLS radiometric calibration as well as the application of the Fuzzy K-means method, proves to be suitable to detect certain types of chemical and biological damages, biological colonization, salts, moisture, etc. in Cultural Heritage.

In order to perform an exhaustive analysis and diagnosis of the structural, chemical and biological damages of constructions, the use of additional measurement techniques (such as visual inspections, NDTs or laboratory tests) are recommended in order to verify results obtained with the TLS approach.

This chapter deals with the use of terrestrial laser scanning for the integral diagnosis and structural analysis of buildings and constructions, from a multisensorial and integrated approach. The main goal is to accurately map and quantify damages of constructions by using this technology. A wide diversity of damage indicators as structural deformations, biological colonization, salt crusts, moisture and black crusts, among others are going to be analyzed from the proposed multisensor strategy. To this end, we propose a non-intrusive semiautomatic methodology through which to study all processes of degradation suffered by the structure.

Under this basis, the present chapter attempts to demonstrate the applicability of the multisensory strategy based on TLS technology in the Master Gate of San Francisco (Figure 1). This historical construction is one of the most representative buildings inside the Restoration fortress of Almeida in Portugal. The Almeida Fortress, is an Italian trace construction conceived to defend the Portuguese border against the Spanish and French invasions during the 17th century (Figure 1 a). For more information about its history and architecture see Arce Campos et al. (Arce et al. 2018) and Sánchez-Aparicio et al. (Sánchez-Aparicio et al. 2018).

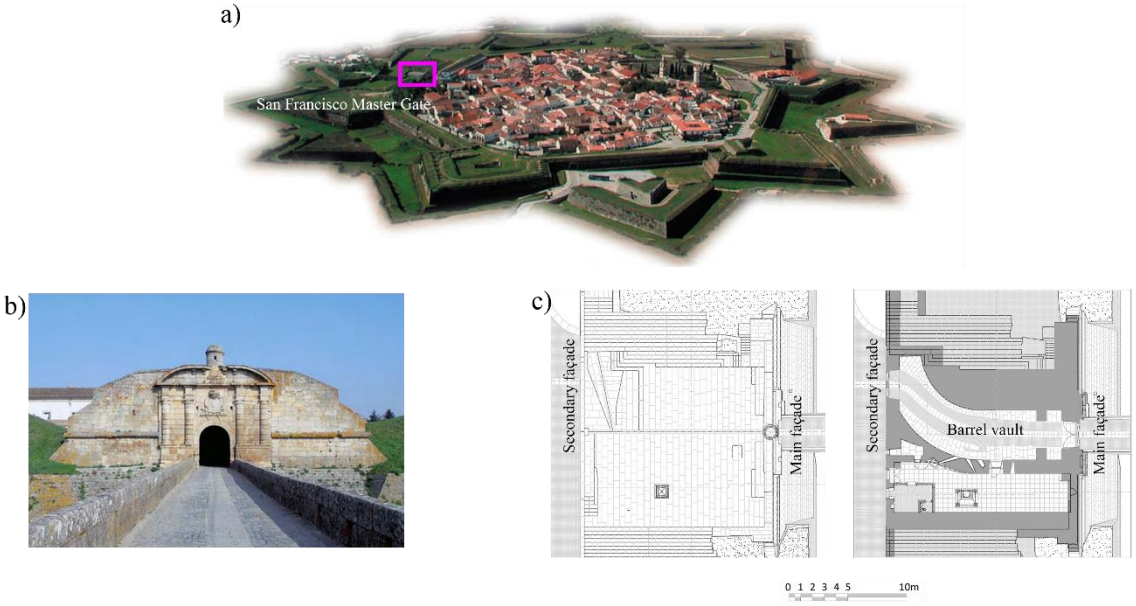

Figure 1: The Almeida fortress: a) aerial view of the fortress adapted from (Cobos and de Sousa Campos 2013) and; b) general view of the Master Gate of San Francisco, adapted from (Cobos and de Sousa Campos 2013) and; c) plant view of the Master Gate of San Francisco.

The chapter is organized as follows: Section 2 presents TLS technology as a suitable support tool to analyze the state of conservation of constructions describing the data acquisition and preprocessing steps required to take full advantage of this technology; Section 3 exposes the results of the construction diagnosis as well as the structural analysis of its current state of conservation

complemented by predictive evaluations; and finally, Section 4 includes the conclusions arising from the use of this technology to succeed documentation, reconstruction and conservation state analysis of most common damages of historical constructions.

2 TLS AS A SUPPORT TOOL TO DIAGNOSE THE CONSERVATION STATE OF CONSTRUCTIONS

The current section will show the methodology proposed and applied to the study case. As Figure 2 illustrates a first visual inspection is necessary and key to determine wich methods an instrumentation will be used. Assuming TLS the best technology to acquire in a non-invasive way large amount of geometric and radiometric information about constructions, we explain this approach first. After TLS data acquisition, the processing of geometric and radiometric data is explained. In this process, different processing algorithms are suggested in order to obtain suitable results. Finally other complementary approaches are described and analyzed with the aim of improve the final structural analysis and diagnosis of constructions.

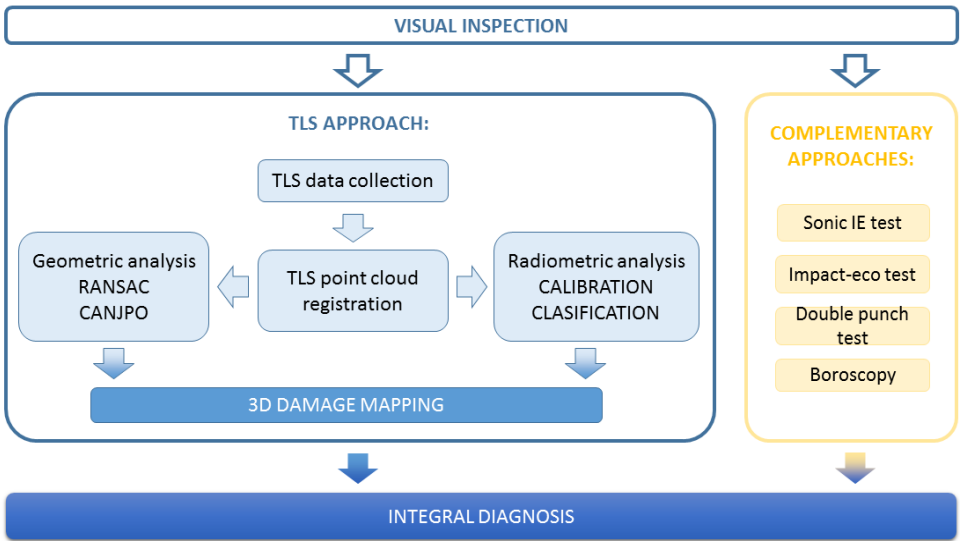

Figure 2: Proposed workflow to perform accurate diagnosis of constructions on the basis of TLS technology.

2.1 **Visual inspection**

Previously to the multisensor campaign, a visual inspection of the construction was required to select the most appropriated methodology to study the current state of conservation of the construction. Since some indicators of damage were observed (white and black crusts, lichens as well as material losses) (Figure 3), it was decided to use a multisensor methodology by using (i) a lightweight terrestrial laser scanner to digitalize the construction as well as to map the different damage presented on it; (ii) some sonic, impact-eco and double punch tests to characterize the

mechanical properties of the masonry; (iii) some impact-eco tests to evaluate the thickness of the supports and; (iii) some boroscopic tests to evaluate the inner composition of the construction.

Figure 3: Current state of conservation of the Master Gate: a) main façade on which is possible to observe the strong biological colonization (orange lichens); b) detail of the current state of the barrel vault with presence of black and white crusts and; c) detail of the material losses in the lower part of the supports.

It should be mentioned that during the visual inspection a close relationship between the material losses of the barrel vault and the presence of some biological and chemical pathologies was observed. Black crusts indicates a polluted atmosphere that promotes the disaggregation of the masonry blocks. These damage process is also linked with the emergence of white crusts due to the hidratation and deshidratation cycles of the melting salts.

2.2 **TLS point cloud: data collection and point cloud processing**

Given the great potential of TLS technology to carry out 3D surveys of any object in a non-invasive way, this technology is rated as one of the most suitable to reconstruct and document historical constructions as well as to study possible deteriorations suffered over time . Besides, this technology offers a great flexibility in data capture and a good level of precision in 3D coordinate measurements, this active-contact-free technology can also record a set of complementary

spectral information, the so called intensity values. Most TLS devices are equipped with an external digital camera, so additional RGB information can be used to compose a photorealistic model of the historical construction.

The TLS most commonly used for the inspection of historical constructions are time-of-flight and phase-shift scanners. While time-of-flight operating principle offer greater precision and longer measurement ranges by a slower data collection, phase-shift devices offer a faster data acquisition.

To analyze the state of deterioration of the Master Gate of San Francisco, it was decided to use a phase-shift TLS, specifically the FaroFocus3D 120 (Figure 4). This TLS device operates at the wavelength of 905 nm and measures distances in the range of 0.60-120 m with a point measurement rate of 976,000 p/s and a nominal precision of ±2 mm at 25 m.

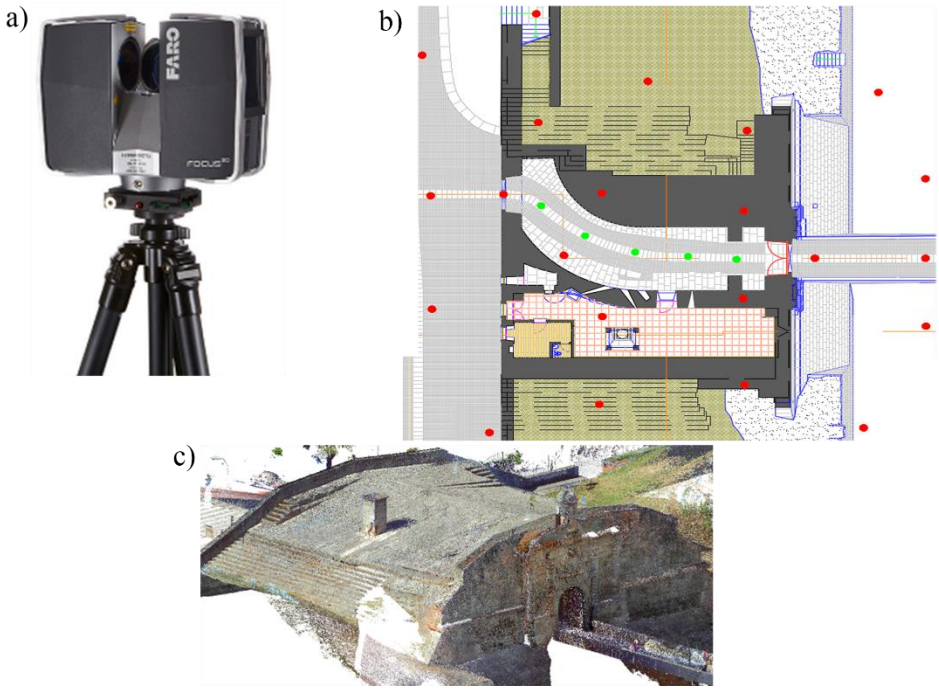

Figure 4: TLS campaign: a) Faro Focus3D 120 scanner; b) Scheme of the data collection network and c) The final 3D photo-realistic model of the Master Gate of San Francisco. The yellow dots represents scan stations carried out to capture de external envelop and the green dots represents scan stations of the barrel vault.

Given the complexity of the case study chosen, especially because of its magnitude (around 689 m^2 in plant) and its complex geometry, a large number of scan stations were required to properly document the entire structure. In this regard, the lightness of the FaroFocus3D sensor allowed to easily perform the data acquisition since 26 scan stations were required to document the entire

construction: 11 for each of the two façades, 5 for the barrel vault and 10 for the roof of the structure. The registration of the different point clouds was carried out by means of the Iterative Closest Point algorithm (Besl and McKay 1992). Thus, a point cloud of 712 million points was obtained after the alignment process using the FaroFocus3D processing software, SCENE®, with a registration error of 0.0005 ± 0.003 m. The point set had to be simplified guaranteeing a homogenous final 3D model in order to reduce computation time and display the subsequent diagnosis analysis. This procedure was performed applying a decimation filter based on the distance among points. At this stage CloudCompare software was used, setting a threshold of 5 mm (best compromise between resolution and computational costs). As a result, a final sub-sample 3D model of 105 million points was obtained.

2.3 **Geometric analysis of the TLS point cloud**

The 3D point cloud as a cluster of millions of points defined in a Cartesian coordinate system, contains great potential information for the diagnosis of constructions. Under this basis, the following section will describe the results obtained after the application of the RANSAC and CANUPO algorithms over the decimated point cloud of the Master Gate of San Francisco.

Previously. the point cloud of the structure was segmented into its different constructive parts, specifically: (i) the main façade of the construction (called façade A); (ii) the inner façade (called façade B); (iii) the roof and; (iv) the barrel vault. This process was performed through the open-source software CloudCompare.

2.3.1 *RANSAC algorithm*

Nowadays, the deformation analysis of constructions are mainly carried out by means of two approaches (Sánchez-Aparicio et al. 2018): (i) a point to point distance comparison between point clouds of different epochs or (ii) a distance comparison between points and the geometric primitives (basically planes but also cylinders, semispheres, etc) that represent the ideal geometry of the constructive element. For the diagnosis of the current state of conservation of the Master Gate of San Francisco the second approach was applied.

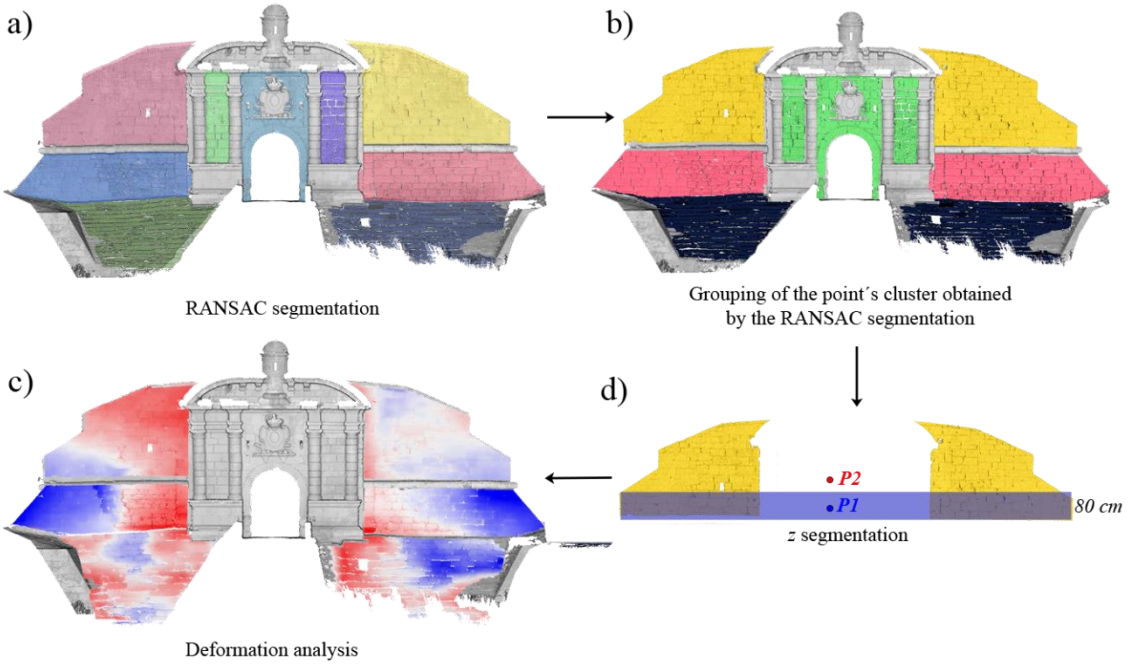

Figure 5: Graphical representation of the approach used to evaluate the possible out-of-plane deformations suffered by the construction. P1 is the centroid of the cluster of points inside the blue rectangle and P2 is the centroid shifted in the *z* axis.

This procedure consists of determining the hypothetical initial state of the constructive element to evaluate deviations suffered over time. For that end, the methodology represented in Figure 5 is proposed. The first stage (Figure 5a) consists of carrying out a RANSAC classification (Schnabel, Wahl, and Klein 2007) in which the TLS point cloud is divided into different groups as representative of each plane. This algorithm is based on the evaluation of the normals of each point and their neighbors. Given that RANSAC provides an excessive number of categorical planes due to spatial discontinuity between some parts of the point cloud, the second strategy (Figure 5 b) tries to unifying groups belonging to similar categorical planes. In order to correctly define the reference planes that belong to each categorical group, it is necessary to carry out a third process. For each of the categorical groups defined in the Figure 5b, a principal component analysis (PCA) is performed using the lower 80 cm (this height corresponds with 2 lines of masonry blocks and will be used as a reference). The results of that process are the centroid of the set of points analyzed (P1) and the maximum dispersion vector (corresponding to the horizontal axis). To define the final reference planes, the maximum dispersion vector and a point (P2) resulting from moving P1 in the vertical direction will be used. Once the final reference planes are determined, the last process consists of mapping the differences between the obtained reference model of the constructive element and the real one. This process is performed by calculating distances between points of the real model and the reference planes (Figure 5d). This procedure

was performed by using Matlab® (Figure 5b and 5c) and the open source software CloudCompare (Figure 5a and 5d).

As a result, it was possible to obtain the deviations between the parametric shape considered as reference (initial state) and the current state captured by the TLS. Being especially useful the data provided by this strategy in the secondary façade and in the roof (Figure 6).

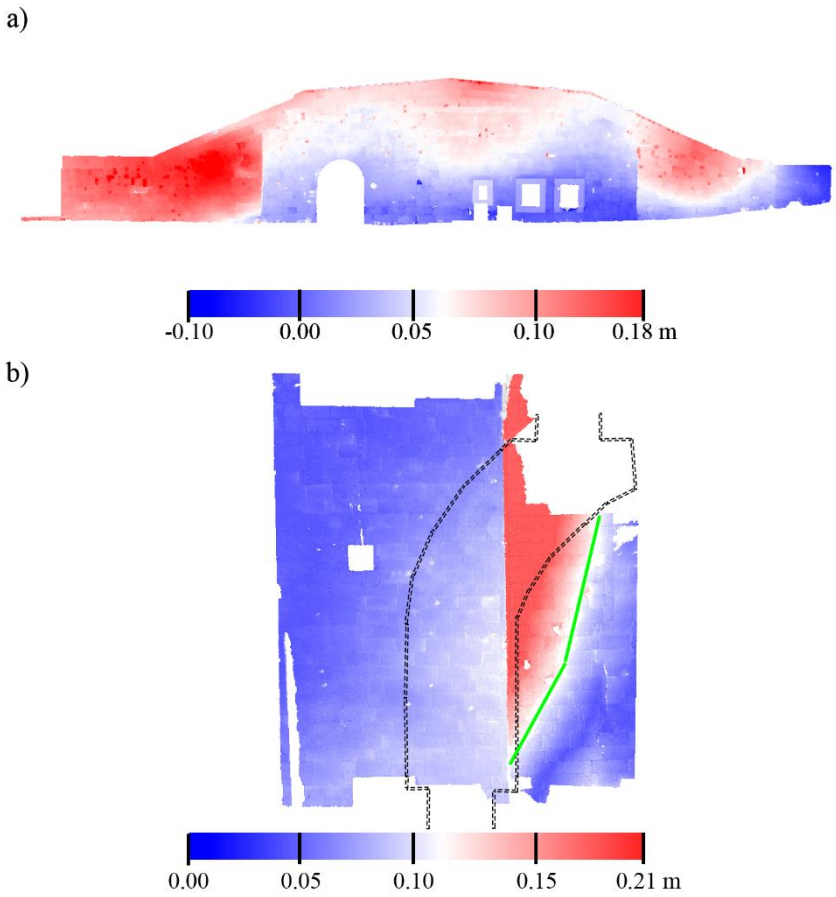

Figure 6: Deformation analysis based on the approach defined by Sánchez-Aparicio et al.; a) secondary façade and; b) the roof. The pseudo-color map was created in the open-source software CloudCompare®. In black dash line the position of the barrel vault and; in green the position of a major crack detected on the roof during the visual inspection.

For further information, see Sánchez-Aparicio et al. (2018).

2.3.2 *CANUPO classifier*

Initially designed for the segmentation of natural spaces, the CANUPO algorithm is a multiscale classification method able to segment point cloud according with the geometrical features contained in its points. To this end, CANUPO classifier evaluates the local dimensionality of each point (Brodu and Lague 2012).

The concept of local dimensionality represents how the point cloud looks like, from a geometrical point of view and at a given location and in a specific scale. To this end, a Principal Component Analysis (eigen-vectors and eigen-values of the covariance matrix) between each point and its neighborhood is carried out, obtaining three eigenvalues ($\lambda_1 > \lambda_2 > \lambda_3$). Then, the variance in dimension is computed following equation 1.

$$p_i = \frac{\lambda_i}{\lambda_1 + \lambda_2 + \lambda_3} \tag{1}$$

where $p_i$is the variance and; λ_i is the eigenvalue evaluated on which i represents the dimension of the eigenvalue evaluated {1,2,3}.

The proportion on which each variance appears can be interpreted as a valid metric to classify the points in different geometrical entities (Figure 7): (i) 1D for those points which correspond to an edge; (ii) 2D for those points which correspond to a planar surface or; (iii) 3D for those points which cannot be classified as 1D or 2D.

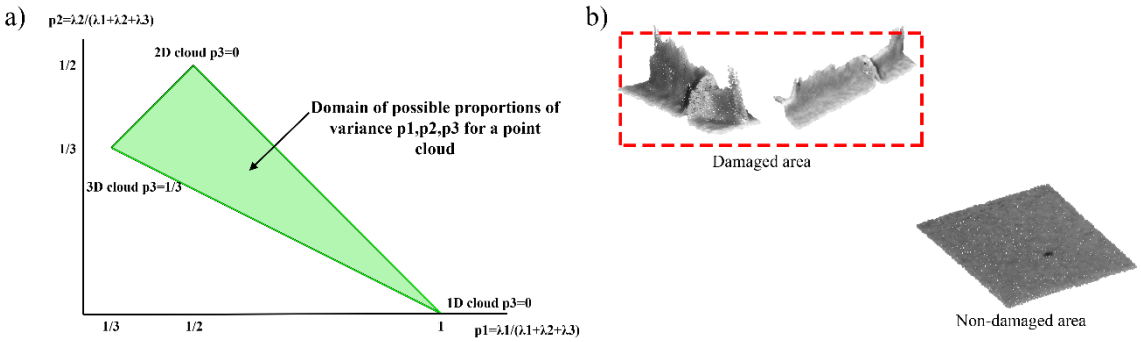

Figure 7: CANUPO classifier: a) classification of the points according with the variance, adapted from(Brodu and Lague 2012) and; b) samples extracted from the Master Gate point cloud and used to train the CANUPO classifier.

Under the basis previously defined, the workflow used for the CANUPO classifier can by summarized in the following stages (Brodu and Lague 2012): (i) the training phase and; (ii) the segmentation stage. During the first stage, the classifier uses the local dimensionality of each point at a different scales to perform a Linear Discriminant Analysis. This analysis allows obtaining the hyperplane of maximal separability between informational classes and thus, the segmentation rule required to classify the point cloud. For the present evaluation, the classifier trained by Sánchez-Aparicio et al. (Sánchez-Aparicio et al. 2018) was used. This classifier was obtained with samples of non-damaged areas and areas characterized by strong material losses coming from the point cloud of the Master Gate. Using a work scale that ranges from a minimum value of 0.05 m to a maximum value of 0.90 m with intervals of 0.05 m. For more information about the threshold definition, please refer to (Sánchez-Aparicio et al. 2018).

Once the segmentation rule was obtained (plane of maximal separability), the barrel vault was segmented into the two informational classes previously defined through the use of the open-source software CloudCompare® (Figure 8).

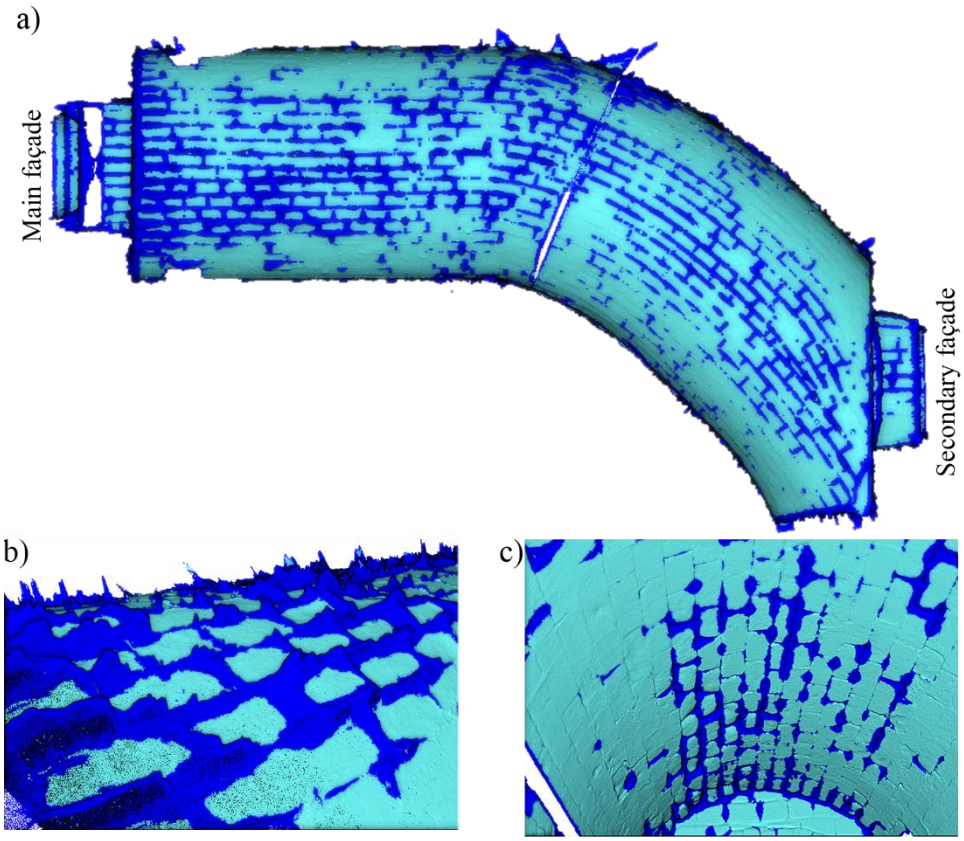

Figure 8: Results obtained with the CANUPO classifier: a) general view of the barrel vault; b) detail of the damages detected by the classifier and; c) inner view of the results obtained.

2.4 **Radiometric analysis of the TLS point cloud**

The backscattered laser intensity data is an added value to the metrics provided by TLS technology. Since the proportion of radiation reflected by each material and for each specific wavelength is different, this information can be used to analyze materials and pathologies. In this way, not only physical but also chemical damages presented in historical constructions could be quantify and monitored over time (Del Pozo et al. 2016). Next, the two main processes required to exploit the radiometric data captured by TLS devices are described.

2.4.1 *Radiometric calibration of the TLS*

TLS detectors receive the backscattered beam laser reflected by each material and then it is converted into an electronic signal proportional to the incoming radiance (Figure 9). So, prior to the radiometric analysis of constructions, a radiometric calibration of the sensor used in data collection is recommended. In this way, reflectance physical values are analyzed instead of digital levels conditioned by the internal alterations of the TLS used in each case. When using TLS technology, this process consists of analyzing the TLS intensity and studying the transformations that take place inside the device and carry out the reversal of such process.

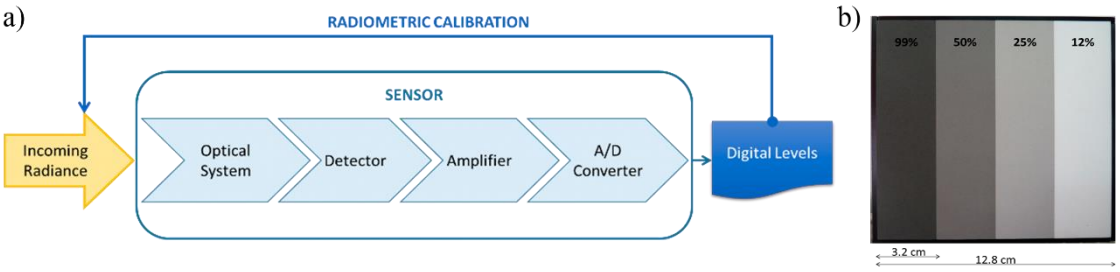

Figure 9: Radiometric calibration of the TLS: a) Transformations of incoming radiance inside TLS sensor and b) the reference panel (Spectralon®) used for the calibration of the FaroFocus3D 120 with four different reflectance panels.

The backscattered TLS signal depends on the distance between the scanner and the measured element and the incoming beam incident angle (Kaasalainen et al. 2011). The distance effect consists of intensity attenuation proportional to square of the distance considered. On the other hand, the incidence angle effect is related not only to the scanning geometry but also to the scattering properties of the surface of the material under study. It affects the backscattered intensity according to the Lambert´s Law so that the higher the incidence angle, the smaller the amount of light coming back to the TLS.

The transformations occur inside the FaroFocus3D 120 were studied for the range of distance between 2 to 36 m. For this range, a logarithmic behavior of the backscattered intensity was obtained and adjusted by the next empirical equation:

$$\rho_{(distance-range)} = e^{a \times b} \times b \times d^2 \times e^{c1 \times I} \quad (2)$$

where *a* and *b* were two coefficients related to the signal attenuation, *d* is the distance, *c1* is the gain of the FaroFocus3D 120 and *I* is the raw intensity value in digital levels (11 bits).

The coefficients related to the signal attenuation have the values shown in the following table for the different ranges of distances.

Table 1: Radiometric calibration coefficients of the FaroFocus3D 120 device.

Range of distances	a	b	c_1	R^2
3-5.25	-1.0928	$3.0295\ 10^{-5}$	0.006397	0.9868
5.25-9	-0.1134	$4.9446\ 10^{-7}$	0.005911	0.9932
9-36	0.0214	$3.9072\ 10^{-7}$	0.005415	0.9966

2.4.2 *Classification algorithm: the fuzzy k-means*

In order to accurately classify the materials of a historical construction as well as it possible chemical damages, the TLS used should be calibrated and so, the point cloud intensity values are reflectances instead of digital levels. Then, a classification process is performed in which each point is classified based on its reflectance value. The two main generic classification approaches are the supervised and unsupervised methods. Table 2 shows the most used classification algorithms.

Table 2: Most common classification techniques. Adapted from (Li et al. 2014).

Classification technique	Characteristics	Examples of classifiers
Pixel-based techniques	Each pixel is assumed pure and typically labelled as a single class	Unsupervised: K-means, ISODATA, SOM, hierarchical clustering

		Supervised: Maximum likelihood, Minimum distance-to-means, Mahalanobis distance, Parallelepiped, K-nearest neighbours. Machine learning: artificial neural network, classification tree, random forest, support vector machine, genetic algorithms.
Sub-pixel-based techniques	Each pixel is considered mixed, and the areal portion of each class is estimated	Fuzzy classification, neutral networks, regression modelling, regression tree analysis, spectral mixture analysis.
Object-based techniques	Geographical objects, instead of individual pixels, are considered the basic unit	Image segmentation and object-based image analysis techniques: E-cognition, ArcGis Feature Analyst.

Below, Figure 10 shows the classification result of a historical construction applying the fuzzy k-means unsupervised approach. This classification was carried out in the software Matlab®.

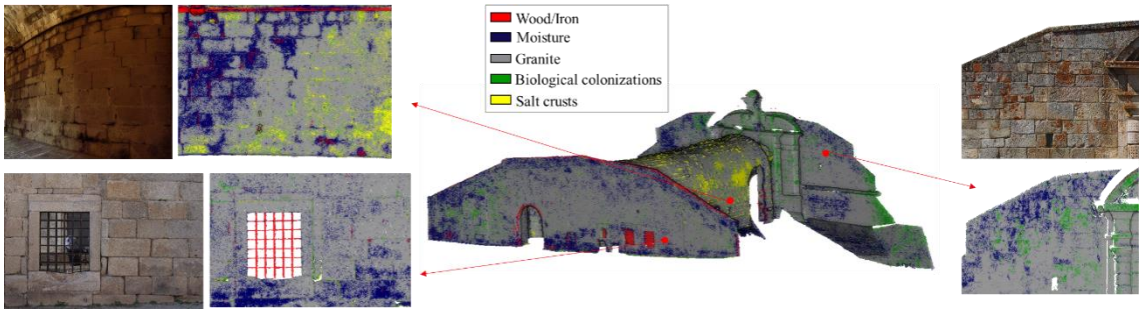

Figure 10: Results obtained after the application of the unsupervised fuzzy k-means algorithm.

2.5 **Additional sensors to complement the diagnosis**

Thanks to the application of the approaches shown in previous sections (Section 2.3 and Section 2.4) it has been possible to characterize great part of damages presented on the construction. Indicators from which a great material losses is deduced. These areas need to be analyzed carefully in order to understand the current stability of the barrel vault. To this end, it was required the use of additional strategies with the aim of complementing the information obtained by the TLS, namely (Figure 11): (i) two indirect sonic tests for the mechanical characterization of the granite used to build the construction, obtaining an average P wave of 1475 m/s and an average R wave of 758 m/s; (ii) six impact-eco tests for the evaluation of thickness support, throwing an average value of 1.77 m; (iii) ten Double Punch tests to evaluate the compressive strength of the mortar

used in the masonry, obtaining a compressive strength of 5.80 MPa and; (iv) one boroscopic test to evaluate the inner composition of the construction.

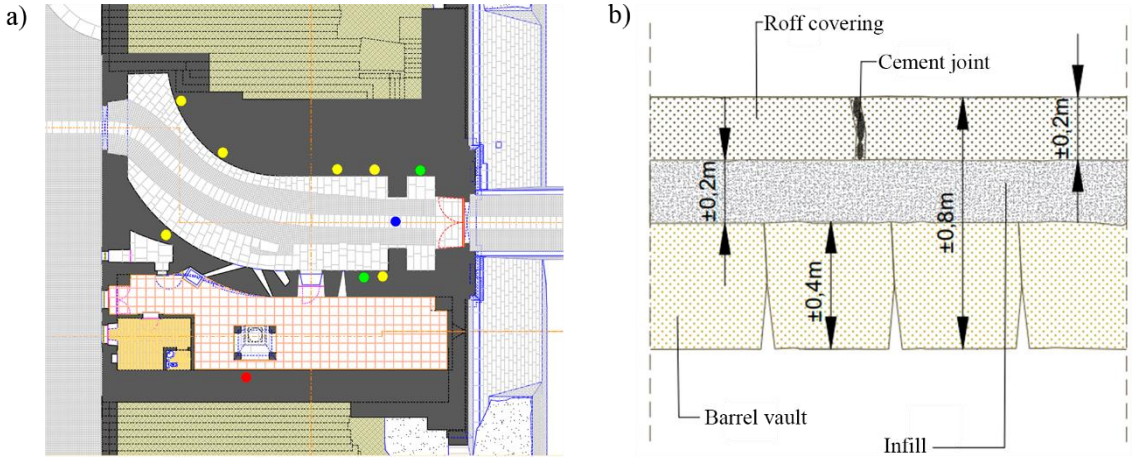

Figure 11: Additional sensors used to complement the diagnosis: a) location of the complementary tests carried out in the Master Gate and; b) results obtained from the boroscopic test carried out. In yellow, the impact-eco tests; in green the places on which the sonic tests were carried out; in red the location on which the mortar specimens were extracted for the Double Punch Tests and; in blue the position on which the boroscopic tests was performed.

For more details about the physical and operational fundaments of these the reader is referred to specialized bibliography (Miranda et al. 2012, Matysek, Seręga, and Kańka 2017).

3 DIAGNOSIS OF THE CONSTRUCTION

According with the results provided by the visual inspection, a diagnosis of the construction is required in order to evaluate the current conservation state. This diagnosis was carried out at two levels: i) analysis of the indicator of damage and; ii) evaluation of the current and future structural stability of the barrel vault.

3.1 **Analysis of the indicators of damage presented on the different constructive elements**

Starting from the results obtained during the application of the different algorithms proposed in the present chapter, a robust 3D damage mapping was carried out (Figure 8)(Figure 10), using to this end the open-source software Cloud Compare®.

Considering the result of this 3D mapping, it was possible to conclude that most preoccupant indicator of damage is the material disaggregation, appearing in the 8.45 % of the total area of the barrel vault (Figure 8) and whose origin can be attributed to the presence of melting salts and

black crusts (Figure 10). With respect to the melting salts, which represents the 4.14% of the total surface of the barrel vault, these compounds can be attributed to possible salts infiltrations coming from the soil as well as the roof covering (made with cement mortar joints) (Figure 11). Regarding the black crusts/moisture, it was possible to observe a presence of this damage in the 14.17% of the barrel vault. These damages are linked with the large amount of biological colonization (orange nitrophylic lichens that colonizes the 4.14% of the façades) (Figure 10). This type of lichens has developed an extra resistance to those environments rich in NO_x, a chemical compound that can be attributed to polluted environments.

Regarding the deformation of the façades, it was not observed the presence of any out-of-plane collapse mechanism (Figure 6). Attributing the deviation to construction defects or derived from the intensive history of the construction, especially for the works carried out in 1986 (Sánchez-Aparicio et al. 2018). Regarding the roof´s deformation (Figure 6b), the discrepancies observed, with a maximum value of 0.21 m, can be attributed to a possible accommodation of the infill, explaining the presence of the large longitudinal crack observed during the visual inspection (Sánchez-Aparicio et al. 2018).

3.2 **Evaluation of the current structural stability**

In contrast with other structural systems such as the concrete or steel-based structures, traditional masonry structures were conceived to support vertical loads (mainly gravity loads). Being its structural integrity a problem of equilibrium more than a problem of resistance (Heyman 1966). Taking this into account, the present section will evaluate the structural stability of the barrel vault (construction element with more conservation problems) under the basis of the discrete limit analysis for masonry construction initially defined by Livesley (Livesley 1978). This approach, conceived for the estimation of the stability of the arches, can be extended for the evaluation of masonry barrel vaults. In this case, the barrel vault is considered as a finite succession of arches along a specific path and thus, the stability of this constructive element depends on the stability of each arch (Heyman 1966).

Taking this into consideration, the first step required for the evaluation of the barrel vault pass through the choice of the most critical arches. Understanding it, as those arches with less resistance section and thus, with more probability of failure by equilibrium (the truss line cannot be contained into the geometry of the arch) or resistance (local stresses higher than the compression strength of the material). Under this basis, and considering the disposition of the different constructive elements, as well as the data provided by the CANUPO classifier, two sections were evaluated of the most damaged part of the structure were evaluated (Figure 12): i) one section in

the vicinity of the intersection with the main façade, this section corresponds with the most damaged section of all the barrel vault and; (ii) one section at the mid-spam of the barrel vault. These sections were extracted with the open-source software CloudCompare and vectorized in the software AutoCAD®.

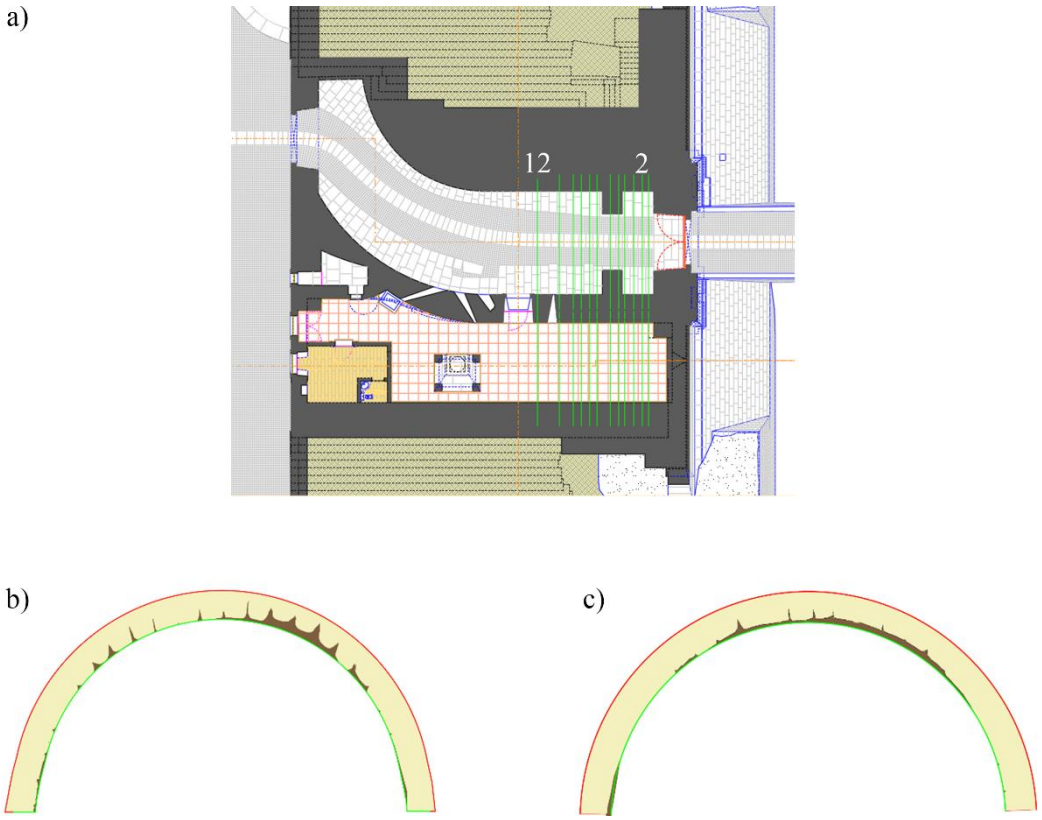

Figure 12: Sections used to evaluate the stability of the barrel vault: a) plant view, b) detail of section 2 and; c) detail of section 12. In red the intrados of the arches and supports, in green the extrados of the initial geometry, in light brown the current section and, in dark brown the estimated material losses.

Once the different sections have been extracted, the next step required for the evaluation of its stability pass through the limit analysis of each arch. To this end, the commercial software limit state RING® was used. This software allows the evaluation of the stability of masonry arches through the use of an improved version of the discrete limit analysis proposed by Livesley (Livesley 1978) on which is possible to consider additional effects such as the sliding between blocks (with or without dilatancy) or the failure by crushing (Gilbert and Melbourne 1994). Complementary to the approach previously defined, the following assumptions were considered in order to simulate the stability of the structure (Table 3) (Figure 13): (i) each arch was simulated according with their effective thickness; (ii) the lack of material in each joint was simulated in order to take into account the reduction of the contact area; (iii) the compressive strength of the

model considered was the strength obtained by means of the double punch test carried out on the mortar, assuming a value of 5.80 MPa; (iv) a frictional model was taken into account in order to simulate possible sliding problems, this model considered a frictional coefficient of 0.6; (v) a Mohr-Coulomb failure criterion was taken into account for the simulation of the infill, assuming a cohesion value of 30 KPa and a frictional angle of 30º; (vi) a Boussinesq load distribution model with a limitation angle of 30º was considered in order to simulate the dispersion of the loads inside the infill of the construction and; (vi) a live load of 5 kN/m was applied on the structure in order to simulate the possibility of having a dense group of people reunited and locate on the top of the structure. This load was considered since each year, in Almeida, a representation of the battle between France and Portugal is carried out (Arce et al. 2018).

Table 3: Effective sections (thickness) used to simulate the generalized material loss presented on the arches.

Section	Initial thickness (mm)	Effective thickness (mm)	Reduction (%)
2	400	343	14.3
12	400	366	8.5

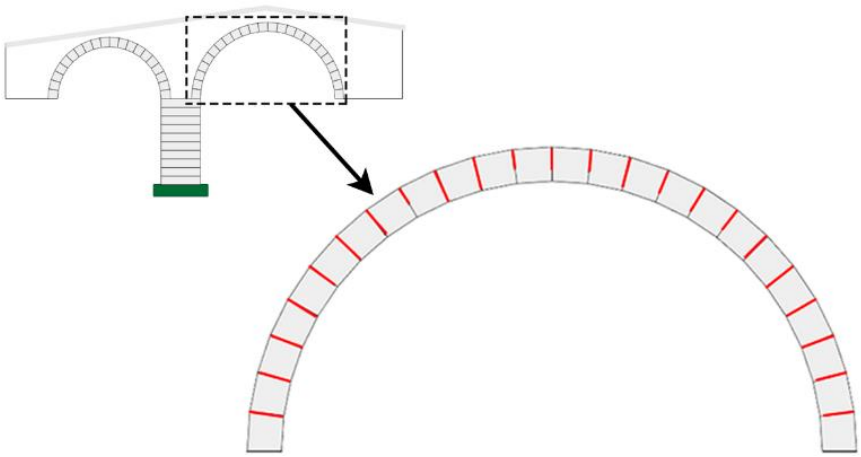

Figure 13: Structural model used to simulate the stability in section 12. In red it is possible to observe the real damage of the barrel vault.

In general terms, and in contrast with the strong material losses presented in the structure, the barrel vault shows large values of stability (Table 4). Showing a minimum safety factor of 7.42 in the union with the main façade (area most affected by the environmental agents) (Figure 14).

Table 4: Results of the structural analysis carried out in section 2 and section 12.

Section	Collapse mechanism	Safety factor (non damaged state)	Safety factor (damaged state)	Safety factor reduction (%)
2	4 plastic hinges	16.90	7.42	43.90
12	4 plastic hinges	16.90	11.50	29.59

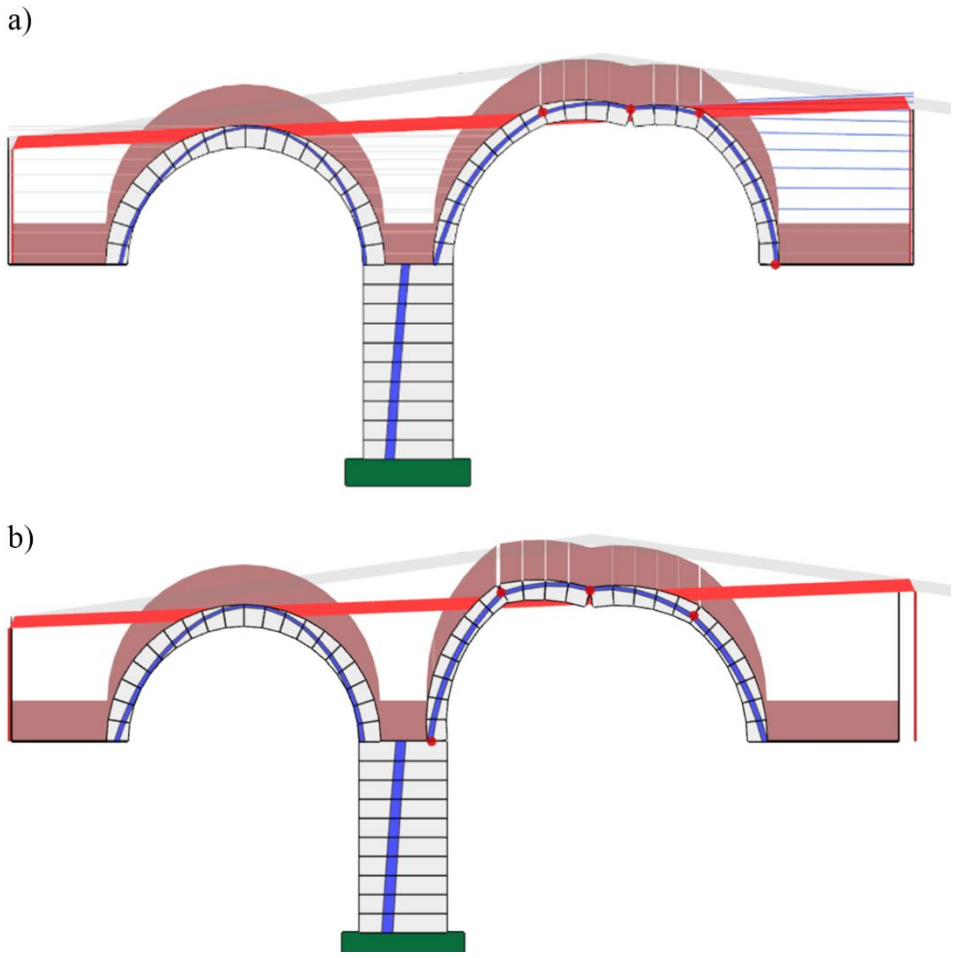

Figure 14: Collapse mechanism of the structure: a) collapse mechanism carried out by the creation of 4 hinges at section 2 and; b) collapse promoted by the formation of 4 hinges at section 12.

3.2.1 *Stability of the construction in case of continuing the material losses*

Taking into account the two possible causes of collapse of the barrel vault: (i) the failure by equilibrium and; (ii) the failure by crushing, seems to be logical that if the material losses continue (as a consequence of the disaggregation of the masonry promoted by the melting salts and the contamination) the structural stability of this construction element will decrease. Under this basis, several predictive evaluations were carried out with the aim of analyzing the influence of dis-

aggregation of the material in the stability of the barrel vault. To this end, several numerical evaluations were carried out, increasing the level of damage in each one (effective section and material losses at joint level) (Table 5).

Table 5: Evolution of the structural stability of the barrel vault with respect to the material losses. Between brackets the structural stability without considering the compressive failure.

Section	Evolution of the safety factors according with the material losses					
	Current	+20%	+40%	+60%	+80%	+100%
2	7.42(11.7)	4.07(6.29)	2.69(5.71)	1.30 (3.02)	-	-
12	11.5(23.9)	9.2(15.7)	6.6(9.9)	5.4(7.7)	3.5 (4.9)	1.09 (3.21)

As expected, if the disaggregation of the masonry blocks continues, the safety factor of the barrel vault decreases as a consequence of the reduction of its resistance section and a reduction of the contact area between elements (equilibrium and resistance failure mechanisms) (Table 5). This value promotes the creation of a collapse mechanism with four hinges and with a similar topology than those obtained previously (Figure 14). According with the results of these numerical evaluations, it is possible to conclude that the most critical part, in terms of stability, is the entrance of the main façade. In this part, if the damage increases in a 65%-70% with respect to the current one, the collapse can be produced in presence of an agglomeration of people on the roof (Table 5). With regards to the medium section of the barrel vault, it is possible to observe higher safety factors at the same increment of the damage (Table 5). The collapse of this part will be produced in a situation on which the level of disaggregation was 200% of the actual damage (Table 5).

It is worth mentioning that for lower levels of disaggregation, the contribution of the compressive strength to the stability of the model is higher than in large levels (Table 5). At medium-high levels of damage the truss line has more problems to be contained inside the arch's limits. However, at high levels of damage (around 180%), the crushing effect (failure by resistance) start to be more important due to the presence of small contact areas, generating high compressive stresses (Table 5).

3.2.2 *Stability of the construction in case of support´s failure*

Apart from the possible reduction of the resistance section of the barrel vault as a consequence of the action of melting salts and traffic contamination, another equilibrium failure can appear as a consequence of a movement of the supports. This type of failure, can be presented in two ways:

(i) as a consequence of loose of the interaction between the infill (passive pressure) and the supports of the barrel vault or; (ii) as a result of the settlement of the supports. Under this basis, additional structural evaluations were carried out.

If the interaction between the infill and the support disappear, the collapse of the arches considered will be promoted by the presence of 4 plastic hinges, three in the main barrel vault and one in the lower part of the main barrel´s support (Figure 15). In this situation the safety factor decreases to a value of 2.29 for the section 2 and value of 6.6 for the section 12. According with this results, and assuming that a recommended safety factor for masonry supports should be 3.0 (Heyman 1966), it is possible to conclude that if the interaction between infill and support disappears, the supports of the entrance, in presence of an agglomeration of people, can suffer some cracks (safety factor lower that 3.0) preserving its stability (safety factor higher than 1.0)(Heyman 1966).

In case of a failure by the settlement of the central support, the structure can collapse as a consequence of a multispam mechanism. This mechanism is composed by a total of eight plastic hinges (four in the main barrel vault and four in the secondary barrel vault) (Figure 15b).

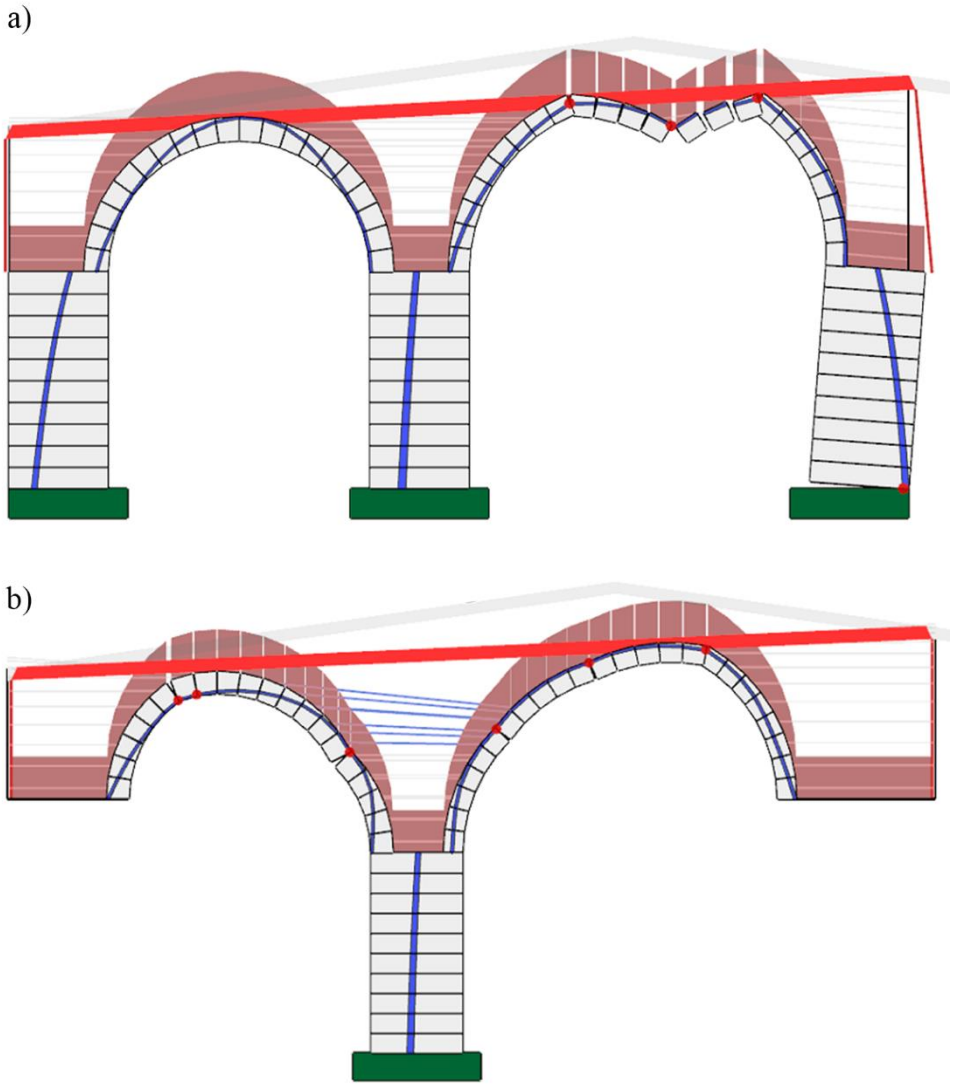

Figure 15: Collapse mechanism as a consequence of the failure of the supports: a) failure of section 2 in case on which the interaction between infill and support disappear and; failure of section 2 in case of settlement of the central support.

4 CONCLUSIONS

Through a selected study case this chapter demonstrates the suitability of TLS point clouds as a support in structural analysis and diagnosis of buildings. Geometric and radiometric procedures have been analyzed in order to assess their properties to guarantee an accurate and meaningful 3D mapping of chemical damages and structural analysis.

Radiometric and geometric TLS data are finally integrated into a multisensory framework that allows an integral diagnosis, being possible to explain the main conservation problem of the study case: the strong material losses. TLS point cloud was used to extract the effective sections of the

most damaged arches of the barrel vault, allowing the evaluation of the current and future structural stability under different casuistic: (i) in case of having more material losses and; (ii) in case of settlement.

By means of the radiometric information provided by TLS, biological and chemical damages were also accurately mapped making it possible a complete pathological diagnosis. For this purpose, we also have point out that the radiometric calibration of the TLS is required, in order to transform the point cloud digital levels into reflectance values. Then, a fuzzy k-means classification algorithm was applied in which each point is classified based on its reflectance value. These pathological processes are linked with the material losses presented on the construction. The black and the white crusts are promoting the material disaggregation (reduction of the resistance section of the barrel vault). The strong biological colonization (nitrophylic lichens) is suggesting the presence of pollutants in the atmosphere which explain the existence of black crusts and thus, the material disaggregation.

With respect to the TLS data acquisition, it is required to take into account the following aspects: (i) the complexity and size of the construction and; (ii) the average density of the point clouds. For the first one, it is recommended the use of a light-weight laser scanner due to the high amount of scan stations needed. Also it would be taken into account the physical principle of the laser, being the time-of-flight scanners the most suitable scanner those constructions on which is not possible to station near the construction (e.g. historical bridges). Concerning the average density of the data acquired, it is recommended the use of a maximum density of 5 mm in order to have a good compromise between resolution and computational costs.

Additional multisensor information coming from indirect sonic tests, impact eco tests, double punch tests and boroscopy inspections, were also used to complement TLS data. The main aim was the mechanical characterization of the granite and mortar used as well as the inner composition between the roof and the barrel vault.

The workflow provided has demonstrated be useful for the evaluation of the current conservation state and the current structural stability of historical constructions. However, the results provided by this methodology can be enhanced in several ways: (i) using additional sensors in order to enhance the separability of the radiometrical calibration, specially between the moisture and black crusts and; (ii) the automatization of the RANSAC approach.

With regards to the study case, and in contrast with the strong material losses, it is possible to conclude that the construction shown enough bearing capacity (safety factor of 7.42). However,

if the material losses continue, the structure can collapse as a consequence of the reduction of the effective section of the barrel vault. The reduction of its effective section depends of the hidratation/deshidration cycles of the melting salts (white crusts) for which would be required the use of additional tests such as Raman spectroscopy or accelerated degradation tests.

In order to avoid a possible collapse of the barrel vault, it is recommended to carry out restoration actions focused on the waterproofing of the roof, the cleaning of the masonry blocks by means of mechanical or laser procedures, the retrofitting of the masonry joints with a compatible mortar as well as traffic restrictions.

REFERENCES

Arce, Andrés, Luís F Ramos, Francisco M Fernandes, Luis Javier Sánchez-Aparicio, and Paulo B Lourenço. 2018. "Integrated structural safety analysis of San Francisco Master Gate in the Fortress of Almeida." *International Journal of Architectural Heritage*:1-18.

Bautista-De Castro, Álvaro, Luis Javier Sánchez-Aparicio, Luís F. Ramos, José Sena-Cruz, and Diego González-Aguilera. 2018. "Integrating geomatic approaches, Operational Modal Analysis, advanced numerical and updating methods to evaluate the current safety conditions of the historical Bôco Bridge." *Construction and Building Materials* no. 158:961-984. doi: https://doi.org/10.1016/j.conbuildmat.2017.10.084.

Besl, Paul J, and Neil D McKay. 1992. "A method for registration of 3-D shapes." *IEEE Transactions on pattern analysis and machine intelligence* no. 14 (2):239-256.

Brodu, Nicolas, and Dimitri Lague. 2012. "3D terrestrial lidar data classification of complex natural scenes using a multi-scale dimensionality criterion: Applications in geomorphology." *ISPRS Journal of Photogrammetry and Remote Sensing* no. 68:121-134.

Cobos, Fernando, and João dos Santos de Sousa Campos. 2013. *Almeida, Ciudad Rodrigo: la fortificación de la Raya Central*: Consorcio Transfronterizo de Ciudades Amuralladas.

Del Pozo, S, LJ Sánchez-Aparicio, P Rodríguez-Gonzálvez, J Herrero-Pascual, A Muñoz-Nieto, D González-Aguilera, and D Hernández-López. 2016. "Multispectral Imaging: Fundamentals, Principles and Methods of Damage Assessment in Constructions." *Non-Destructive Techniques for the Evaluation of Structures and Infrastructure* no. 11:139.

Fernandez-Palacios, Belen Jimenez, Daniele Morabito, and Fabio Remondino. 2017. "Access to complex reality-based 3D models using virtual reality solutions." *Journal of cultural heritage* no. 23:40-48.

Gilbert, Melbourne, and C Melbourne. 1994. "Rigid-block analysis of masonry structures." *Structural engineer* no. 72 (21).

Heyman, Jacques. 1966. "The stone skeleton." *International Journal of solids and structures* no. 2 (2):249-279.

Hori, Y, and T Ogawa. 2017. "Visualization of the construction of ancient roman buildings in ostia using point cloud data." *The International Archives of Photogrammetry, Remote Sensing and Spatial Information Sciences* no. 42:345.

Kaasalainen, Sanna, Anttoni Jaakkola, Mikko Kaasalainen, Anssi Krooks, and Antero Kukko. 2011. "Analysis of Incidence Angle and Distance Effects on Terrestrial Laser Scanner Intensity: Search for Correction Methods." *Remote Sensing* no. 3 (10):2207.

Korumaz, Mustafa, Michele Betti, Alessandro Conti, Grazia Tucci, Gianni Bartoli, Valentina Bonora, Armağan Güleç Korumaz, and Lidia Fiorini. 2017. "An integrated Terrestrial Laser Scanner (TLS), Deviation Analysis (DA) and Finite Element (FE) approach for health assessment of historical structures. A minaret case study." *Engineering Structures* no. 153:224-238. doi: https://doi.org/10.1016/j.engstruct.2017.10.026.

Li, Miao, Shuying Zang, Bing Zhang, Shanshan Li, and Changshan Wu. 2014. "A review of remote sensing image classification techniques: The role of spatio-contextual information." *European Journal of Remote Sensing* no. 47 (1):389-411.

Livesley, RK. 1978. "Limit analysis of structures formed from rigid blocks." *International Journal for Numerical Methods in Engineering* no. 12 (12):1853-1871.

Matysek, Piotr, Szymon Seręga, and Stanisław Kańka. 2017. "Determination of the mortar strength using double punch testing." *Procedia Engineering* no. 193:104-111.

Miranda, Luís Filipe, João Rio, João Miranda Guedes, and Aníbal Costa. 2012. "Sonic Impact Method–A new technique for characterization of stone masonry walls." *Construction and Building Materials* no. 36:27-35.

Sánchez-Aparicio, Luis Javier, Susana Del Pozo, Luís F Ramos, Andrés Arce, and Francisco M Fernandes. 2018. "Heritage site preservation with combined radiometric and geometric analysis of TLS data." *Automation in Construction* no. 85:24-39.

Sánchez-Aparicio, Luis Javier, Belén Riveiro, Diego Gonzalez-Aguilera, and Luís F Ramos. 2014. "The combination of geomatic approaches and operational modal analysis to improve calibration of finite element models: A case of study in Saint Torcato Church (Guimarães, Portugal)." *Construction and Building Materials* no. 70:118-129.

Schnabel, Ruwen, Roland Wahl, and Reinhard Klein. 2007. Efficient RANSAC for point-cloud shape detection. Paper read at Computer graphics forum.

Yang, Hao, Xiangyang Xu, and Ingo Neumann. 2018. "Optimal finite element model with response surface methodology for concrete structures based on Terrestrial Laser Scanning technology." *Composite Structures* no. 183:2-6. doi: https://doi.org/10.1016/j.compstruct.2016.11.012.